

# X(1835), X(2120) and X(2370) in flux tube models

Chengrong Deng<sup>1</sup>, Jialun Ping<sup>2\*</sup>, Youchang Yang<sup>3</sup>, Fan Wang<sup>4</sup>

<sup>1</sup>*School of Mathematics and Physics, Chongqing Jiaotong University, Chongqing 400074, P.R. China*

<sup>2</sup>*Department of Physics, Nanjing Normal University, Nanjing 210097, P.R. China*

<sup>3</sup>*Department of Physics, Zunyi Normal College, Zunyi 563002, P.R. China and*

<sup>4</sup>*Department of Physics, Nanjing University, Nanjing 210093, P.R. China*

Nonstrange hexaquark state  $q^3\bar{q}^3$  spectrum is systematically studied by using the Gaussian expansion method in flux tube models with a six-body confinement potential. All the model parameters are fixed by baryon properties, so the calculation of hexaquark state  $q^3\bar{q}^3$  is parameter-free. It is found that some ground states of  $q^3\bar{q}^3$  are stable against disintegrating into a baryon and an antibaryon. The main components of X(1835) and X(2370), which are observed in the radiative decay of  $J/\psi$  by BES collaboration, can be described as compact hexaquark states  $N_8\bar{N}_8$  and  $\Delta_8\bar{\Delta}_8$  with quantum numbers  $I^G J^{PC} = 0^+0^{-+}$ , respectively. These bound states should be color confinement resonances with three-dimensional configurations similar to rugby ball, however, X(2120) can not be accommodated in this model approach.

PACS numbers: 12.39.Jh, 13.75.Cs, 14.40.Rt

## I. INTRODUCTION

In 2003, X(1860) was observed in the  $p\bar{p}$  invariant mass spectrum in the radiative decay  $J/\psi \rightarrow \gamma p\bar{p}$  by BES collaboration, the mass and the width are  $M = 1859_{-10}^{+3+5}$  MeV and  $\Gamma < 30$  MeV, respectively [1]. In 2005, X(1835) was first observed in  $J/\psi \rightarrow \gamma\pi^+\pi^-\eta'$  decays with a statistical significance of  $7.7\sigma$  by BES-II [2], the parameters of X(1835) are  $M = 1833.7 \pm 6.5 \pm 2.7$  MeV and  $\Gamma = 67.7 \pm 20.3 \pm 7.7$  MeV. Very recently, the X(1835) was confirmed by BES-III in the radiative decay  $J/\psi \rightarrow \gamma\pi^+\pi^-\eta'$  with mass and width  $M = 1836.5 \pm 3.0_{-2.1}^{+5.6}$  MeV and  $\Gamma = 190 \pm 9_{-36}^{+38}$  MeV, respectively [3]. The mass is consistent with the BES-II result, while the width is significantly larger. Meanwhile, X(2120) and X(2370) were also observed in the same process, the masses and the widths are  $M_{X(2120)} = 2122.4 \pm 6.7_{-2.7}^{+4.7}$  MeV,  $M_{X(2370)} = 2376.3 \pm 8.7_{-4.3}^{+3.2}$  MeV,  $\Gamma_{X(2120)} = 83 \pm 16_{-11}^{+31}$  MeV, and  $\Gamma_{X(2370)} = 83 \pm 17_{-6}^{+44}$  MeV, respectively.

Various theoretical works were stimulated to interpret the natures and structures of these resonances. Datta and O'Donnell described X(1860) as a zero baryon number, deuteron-like singlet  $p\bar{p}^0S_1$  state in a simple potential model with a  $\lambda \cdot \lambda$  confining interaction [4]. Ding and Yan discussed X(1860) as a baryonium and investigated mesonic decays of X(1860) due to the nucleon-antinucleon annihilation [5]. Gao and Zhu understood X(1860) as the  $p\bar{p}$  bound state with quantum numbers  $I^G J^{PC} = 0^+0^{-+}$ , and demonstrated that it can not decay into final state  $\pi^+\pi^-$ ,  $2\pi^0$ ,  $\bar{K}K$  and  $3\pi$  [6]. Kochelev and Min explained X(1835) as the lowest pseudoscalar glueball state due to the instanton mechanism of partial  $U(1)_A$  symmetry restoration [7]. He *et al.* studied X(1835) using the QCD sum rule and interpreted it as a

pseudoscalar state with a large gluon content [8]. Li investigated X(1835) as a  $0^{-+}$  pseudoscalar glueball using an effective Lagrangian approach [9]. Ding *et al.* treated X(1835) as a baryonium with a sizable gluon content [10]. Liu proposed that X(1835) contained a baryonium component from the large- $N_c$  QCD point of view [11]. Dedonder *et al.* studied X(1835) in the conventional  $N\bar{N}$  potential model and suggested that it could be a broad and weakly bound state  $N\bar{N}_s(1870)$  in the  $^1S_0$  wave. Huang and Zhu treated X(1835) as the second radial excitation of  $\eta'(958)$  and discussed the strong decay behavior by the effective Lagrangian approach [12]. Li and Ma studied several two-body strong decays of X(1835) associated with  $\eta(1760)$  by the quark-pair-creation model, where X(1835) is assigned as the  $n^{2s+1}L_J = 3^1S_0 q\bar{q}$  state. Entem and Fernández derived a  $N\bar{N}$  interaction from a constituent quark model constrained by the  $NN$  sector to investigate the possible baryonium resonant state X(1835) [13]. Yu *et al.*'s study indicated that: (1) X(1835) could be the second radial excitation of  $\eta'(958)$ ; (2) X(2120) and (2370) can be explained as the third and fourth radial excitations of  $\eta(548)/\eta'(958)$  [14].

Quantum Chromodynamics (QCD) is widely accepted as the fundamental theory to describe the hadron and the strong interaction and has verified in high momentum transfer process. In the low energy region, such as hadron spectroscopy and hadron-hadron interaction study, the *ab initio* calculation directly from QCD becomes very difficult due to the complication of nonperturbative nature. Recently, lattice QCD (LQCD) and nonperturbative QCD method have made impressive progresses on hadron properties, even on hadron-hadron interactions [15–19]. However, QCD-inspired constituent quark model (CQM) is still an useful tool in obtaining physical insight for these complicated strong interaction systems. CQM can offer the most complete description of hadron properties and is probably the most successful phenomenological model of hadron structure [20]. In traditional CQM, a two-body interaction proportional

\*Corresponding author: J. Ping (jlping@njnu.edu.cn)

to the color charges  $\lambda_i \cdot \lambda_j$  and  $r_{ij}^n$ , where  $n = 1$  or  $2$  and  $r_{ij}$  is the distance between two quarks, was introduced to phenomenologically describe quark confinement interaction. The model can automatically prevent overall color singlet multiquark states disintegrating into several color sub-systems by means of color confinement with an appropriate  $SU_C(3)$  Casimir constant [21]. The model also allows a multiquark system disintegrating into color-singlet clusters, and it leads to interacting potentials within mesonlike  $q\bar{q}$  and baryonlike  $qqq$  subsystems in accord with the empirically known potentials [21]. However, the model is known to be flawed phenomenologically because it leads to power law van der Waals forces between color-singlet hadrons [22–26]. It is also flawed theoretically in that it is very implausible that the long-range static multibody potential is just a sum of the two-body ones [21]. The problems are related to the fact that this model does not respect local color gauge invariance [27–30]. Robson proposed to use many-body confinement potentials for meson-meson and baryon-baryon systems [30], which contains the essential features of the solution which emerges from the flux model based on the strong coupling limit of LQCD Hamiltonian and on the explicit local color gauge invariance [31].

QCD does not deny the existence of multiquark states although experimental candidates have not been confirmed up to now. The structures of multiquark systems and hadron-hadron interactions are abundant [32–34], which have important information that is absent in ordinary hadrons, such as  $qq\bar{q}$  and  $qq\bar{q}$  interactions [35]. Recently, LQCD calculations on mesons, baryons, tetraquark and pentaquark states reveal flux-tube or string like structure [36–39]. The confinement of multiquark states are multibody interactions and can be simulated by a potential which proportional to the minimum of the total length of strings which connect the quarks to form a multiquark system. A naive flux-tube or string model basing on this picture has been constructed [32–34]. It takes into account of multibody confinement with harmonic interaction approximation, i.e., where the length of string is replaced by the square of the length to simplify the numerical calculation. There are two arguments to support this approximation: One is that the spatial variations in separation of the quarks (lengths of the string) in different hadrons do not differ significantly, so the difference between the linear and quadratic forms is small and can be absorbed in the adjustable parameter, the stiffness. The calculations on nucleon-nucleon interactions support the argument [32, 40, 41]. The second is that we are using a nonrelativistic description of the dynamics and, as was shown long ago [42], an interaction energy that varies linearly with separation between fermions in a relativistic, first order differential dynamics has a wide region in which a harmonic approximation is valid for the second order (Feynman-Gell-Mann) reduction of the equations of motion.

The flux tube model has been applied to the study of

exotic mesons [33]. The results suggest that the multibody confinement should be employed in the quark model study of multiquark systems instead of the additive two-body confinement. The flux tube model with four-body confinement potential also described light scalar meson spectrum well in the framework of a tetraquark picture [43]. This paper extends the model to hexaquark  $q^3\bar{q}^3$  system, to investigate systematically the non-strange baryonium states with six-body confinement potential. The numerical results are obtained by Gaussian Expansion Method (GEM) [44]. The paper is organized as follows: the model Hamiltonian and wavefunction for 3-quark system are presented in Sec. II. The six-body confinement potential and the wavefunction of a hexaquark system are introduced in Sec. III. Sect. IV presents the numerical results and discussions. A brief summary is given in the last section.

## II. QUARK MODELS AND MODEL PARAMETERS

The non-relativistic quark model was formulated under the assumption that the hadrons are color singlet non-relativistic bound states of constituent quarks with phenomenological effective masses and interactions.

### A. Isgur-Karl model

Isgur-Karl model incorporating effective one gluon exchange (OGE) and confinement potentials successfully describe the properties of baryon spectrum [45–47]. The model Hamiltonian used for baryons takes the form

$$H = \sum_{i=1}^3 \left( m_i + \frac{\mathbf{p}_i^2}{2m_i} \right) - T_{CM} + \sum_{i>j}^3 V_{ij}^G + V^C, \quad (1)$$

$$V_{ij}^G = \frac{1}{4} \alpha_s \lambda_i \cdot \lambda_j \left[ \frac{1}{r_{ij}} - \frac{\pi}{2} \delta(\mathbf{r}_{ij}) \right. \\ \left. \times \left( \frac{1}{m_i^2} + \frac{1}{m_j^2} + \frac{4}{3m_i m_j} \sigma_i \cdot \sigma_j \right) \right], \quad (2)$$

$$V^C = \frac{K}{3} [(\mathbf{r}_1 - \mathbf{r}_2)^2 + (\mathbf{r}_1 - \mathbf{r}_3)^2 + (\mathbf{r}_2 - \mathbf{r}_3)^2], \quad (3)$$

the confinement potential  $V^C$  can also be written as

$$V^C = K \left[ \left( \frac{\mathbf{r}_1 - \mathbf{r}_2}{\sqrt{2}} \right)^2 + \left( \frac{\mathbf{r}_1 + \mathbf{r}_2 - 2\mathbf{r}_3}{\sqrt{6}} \right)^2 \right]. \quad (4)$$

When the model is extended to study multiquark states [48], the confinement can be equivalently expressed as

$$V^C = \sum_{i>j}^n -a_c \lambda_i \cdot \lambda_j r_{ij}^2. \quad (5)$$

Where  $T_{CM}$  is the center-of-mass kinetic energy,  $\mathbf{r}_i$ ,  $m_i$  and  $\mathbf{p}_i$  are the position, mass and momentum of the  $i$ -th quark,  $\lambda$  and  $\sigma$  are the  $SU(3)$  Gell-man and  $SU(2)$  Pauli matrices, respectively. Note that  $\lambda \rightarrow -\lambda^*$  for anti-quark. All other symbols have their usual meaning. An effective scale-dependent strong coupling constant [49] is used here

$$\alpha_s(\mu) = \frac{\alpha_0}{\ln \left[ \frac{\mu^2 + \mu_0^2}{\Lambda_0^2} \right]} \quad (6)$$

where  $\mu$  is the reduced mass of two interactional quarks, and  $\alpha_0$ ,  $\mu_0$  and  $\Lambda_0$  are determined below. The  $\delta$  function, arising as a consequence of the non-relativistic reduction of the one-gluon exchange diagram between point-like particles, has to be regularized in order to perform numerical calculations. It reads [50]

$$\delta(r_{ij}) = \frac{1}{\beta^3 \pi^{\frac{3}{2}}} e^{-r_{ij}^2/\beta^2} \quad (7)$$

where  $\beta$  is the model parameter which is determined by fitting the experiment data.

## B. Chiral quark model

The  $SU(2) \times SU(2)$  chiral quark model described  $NN$  phase shifts and the properties of deuteron quite well [51–53]. Subsequently, the  $SU(3) \times SU(3)$  chiral quark model where constituent quarks interact only through pseudoscalar Goldstone bosons exchange (GBE) was developed to describe the baryon spectra [54]. The model including both OGE and GBE was successfully applied to the  $NN$  and nucleon-hyperon interactions [55–57]. The Goldstone bosons exchange potentials can be expressed as,

$$V_{ij}^B = v_{ij}^\pi \sum_{a=1}^3 \mathbf{F}_i^a \mathbf{F}_j^a + v_{ij}^K \sum_{a=4}^7 \mathbf{F}_i^a \mathbf{F}_j^a + v_{ij}^\eta (\mathbf{F}_i^8 \mathbf{F}_j^8 \cos \theta_P - \mathbf{F}_i^0 \mathbf{F}_j^0 \sin \theta_P), \quad (8)$$

$$v_{ij}^\chi = \frac{g_{ch}^2}{4\pi} \frac{m_\chi^3}{12m_i m_j} \frac{\Lambda_\chi^2}{\Lambda_\chi^2 - m_\chi^2} \boldsymbol{\sigma}_i \cdot \boldsymbol{\sigma}_j \left[ Y(m_\chi r_{ij}) - \frac{\Lambda_\chi^3}{m_\chi^3} Y(\Lambda_\chi r_{ij}) \right], \chi = \pi, K, \eta, \quad (9)$$

$$V_{ij}^\sigma = -\frac{g_{ch}^2}{4\pi} \frac{\Lambda_\sigma^2}{\Lambda_\sigma^2 - m_\sigma^2} m_\sigma \left[ Y(m_\sigma r_{ij}) - \frac{\Lambda_\sigma}{m_\sigma} Y(\Lambda_\sigma r_{ij}) \right].$$

where  $Y(x)$  is the standard Yukawa functions defined by  $Y(x) = \frac{e^{-x}}{x}$  and  $\mathbf{F}^a$  is flavor  $SU(3)$  Gell-mann matrices. The angle  $\theta_P$  appears as a consequence of considering the physical  $\eta$  instead of the octet one.  $m_\pi$ ,  $m_K$  and  $m_\eta$  are the masses of the  $SU(3)$  Goldstone bosons, took their experimental values.  $m_\sigma$  is determined through the PCAC relation  $m_\sigma^2 \sim m_\pi^2 + 4m_{u,d}^2$  [58]. The chiral coupling constant  $g_{ch}$  is determined from the  $\pi NN$  coupling

constant through

$$\frac{g_{ch}^2}{4\pi} = \left( \frac{3}{5} \right)^2 \frac{g_{\pi NN}^2}{4\pi} \frac{m_{u,d}^2}{m_N^2} \quad (10)$$

Here the flavor  $SU(3)$  is assumed to be an exact system and only broken by the different mass of the strange quark. The confinement and OGE interaction terms are the same as those of Isgur-Karl model and will not be rewritten here.

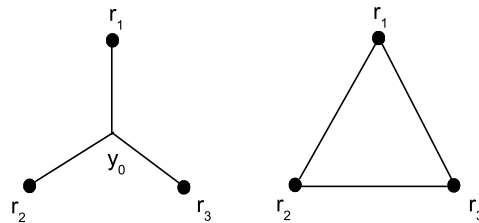


FIG. 1: Three-body and two-body confinement potential

## C. Flux-tube model

This model assumption is inspired by the LQCD calculation. LQCD calculations for baryons reveal flux-tube or string like structure [37, 59]. The simplified version, Y-shape structure, is shown in Fig. 1, where the  $\mathbf{r}_i$  represents the spatial position of the  $i$ -th quark denoted by a black dot and  $\mathbf{y}_0$  denotes the junction where three color flux tubes meet. The confinement is proportional to the minimum of the sum of the square of the length of three flux tubes. In the flux tube model with quadratic potential, the three-body confinement can be written as

$$V^C = K [(\mathbf{r}_1 - \mathbf{y}_0)^2 + (\mathbf{r}_2 - \mathbf{y}_0)^2 + (\mathbf{r}_3 - \mathbf{y}_0)^2] \quad (11)$$

For the confinement potential  $V^C$ , the position of the junction  $\mathbf{y}_0$  can be fixed by minimizing the energy of the system, then we get

$$\mathbf{y}_0 = \frac{\mathbf{r}_1 + \mathbf{r}_2 + \mathbf{r}_3}{3} \quad (12)$$

Therefore, the minimum of the confinement potential for baryons  $V_{min}^C$  has the following forms

$$V_{min}^C = K \left[ \left( \frac{\mathbf{r}_1 - \mathbf{r}_2}{\sqrt{2}} \right)^2 + \left( \frac{2\mathbf{r}_3 - \mathbf{r}_1 - \mathbf{r}_2}{\sqrt{6}} \right)^2 \right]. \quad (13)$$

The other parts of Hamiltonian of flux tube model are the same as Isgur-Karl model (denoted as Model I hereafter) or chiral quark model (Model II). It should be noted that for a baryon the three-body quadratic confinement potential is exactly equivalent to the sum of two-body one,

$\Delta$ -shape in Fig. 1 (although it is not exactly the case for the linear confinement potential). As far as baryon is concerned, the flux tube model is not a new model. However, when it is applied to multi-quark systems, the flux-tube confinement potential is different from the traditional two-body confinement ((Isgur-Karl model and chiral quark model) [32–34]).

In this work, the tensor forces and spin-orbit forces between quarks are omitted in three models, because of their small or zero contributions to the ground state baryons.

#### D. Wavefunctions and baryon spectrums

For baryons, the color part wavefunction  $\psi_c$  is antisymmetrical because of the color singlet requirement. The spatial wavefunction  $\psi_{L_T M_T}^G(\mathbf{R}, \mathbf{r})$  is assumed to be symmetrical because we are interested in ground states. So the spin-flavor wavefunction  $\psi_{I M_I S M_S}$ , the  $SU(6) \supset SU_s(2) \times SU_f(3)$  symmetry is used here, is symmetrical under the exchange of two identical particles. The total antisymmetrical wavefunction can be described as,

$$\Phi_{I M_I J M_J}(\mathbf{R}, \mathbf{r}) = \psi_c [\psi_{L_T M_T}^G(\mathbf{R}, \mathbf{r}) \psi_{I M_I S M_S}]_{I M_I J M_J}. \quad (14)$$

$[\dots]_{I M_I J M_J}$  means coupling the spin  $S$  and total orbital angular momentum  $L_T$  with Clebsch-Gordan coefficients.

We define Jacobi coordinates  $\mathbf{r}_{ij}$  and  $\mathbf{R}_k$  for the cyclic permutations of (1, 2, 3),

$$\mathbf{r}_{ij} = \mathbf{r}_i - \mathbf{r}_j, \quad \mathbf{R}_k = \mathbf{r}_k - \frac{m_i \mathbf{r}_i + m_j \mathbf{r}_j}{m_i + m_j}. \quad (15)$$

Then, the spatial symmetrical wavefunctions can be expressed as,

$$\Psi_{L_T M_T}(\mathbf{R}, \mathbf{r}) = \sum_{i,j,k=1}^3 [\phi_{lm}(\mathbf{r}_{ij}) \phi_{LM}(\mathbf{R}_k)]_{L_T M_T}, \quad (16)$$

$\phi_{lm}(\mathbf{r}_{ij})$  and  $\phi_{LM}(\mathbf{R}_k)$  are the superpositions of Gaussian basis functions with different sizes,

$$\phi_{lm}(\mathbf{r}_{ij}) = \sum_{n=1}^{n_{max}} c_n N_{nl} r_{ij}^l e^{-\nu_n r_{ij}^2} Y_{lm}(\hat{\mathbf{r}}_{ij}), \quad (17)$$

$$\psi_{LM}(\mathbf{R}_k) = \sum_{N=1}^{N_{max}} c_N N_{NL} R_k^L e^{-\nu_N R_k^2} Y_{LM}(\hat{\mathbf{R}}_k), \quad (18)$$

where  $N_{nl}$  and  $N_{NL}$  are normalization constants. Gaussian size parameters  $\nu_n$  and  $\nu_N$  are taken as geometric progression,

$$r_n = r_1 a^{n-1}, \quad \nu_n = \frac{1}{r_n^2}, \quad a = \left( \frac{r_{n_{max}}}{r_1} \right)^{\frac{1}{n_{max}-1}}, \quad (19)$$

$$R_N = R_1 A^{N-1}, \quad \nu_N = \frac{1}{R_N^2}, \quad A = \left( \frac{R_{N_{max}}}{R_1} \right)^{\frac{1}{N_{max}-1}} \quad (20)$$

The numbers  $n$  and  $l$  ( $N$  and  $L$ ) specify the radial and angular momenta excitations with respect to the Jacobi coordinates  $\mathbf{r}(\mathbf{R})$ , respectively. The angular momenta  $l$  and  $L$  are coupled to the total orbit angular momentum  $L_T$ . In the present work all three angular momenta are assumed to be zero.

Using above Hamiltonian and wavefunctions, the light baryon spectra and the corresponding model parameters can be obtained by solving the three-body Schrödinger equation

$$(H_3 - E)\Phi_{I M_I J M_J}(\mathbf{R}, \mathbf{r}) = 0 \quad (21)$$

with Rayleigh-Ritz variational principle. The converged results, which are shown in Table I, are arrived by setting  $r_1 = R_1 = 0.3$  fm,  $r_{n_{max}} = R_{n_{max}} = 2.0$  fm and  $n_{max} = N_{max} = 5$ . It can be seen from Table I that Isgur-Karl model and chiral quark model give similar numerical results, which can describe well the light baryon spectrum. The fitting parameters in Isgur-Karl model

TABLE I: Baryon spectra (unit: MeV).

State	N	$\Lambda$	$\Sigma$	$\Xi$	$\Delta$	$\Sigma^*$	$\Xi^*$	$\Omega$
Isgur-Karl	939	1022	1196	1307	1232	1397	1542	1673
Chiral	939	1048	1249	1375	1232	1391	1536	1670
Expreiment	939	1116	1195	1315	1232	1384	1533	1672

TABLE II: Model parameters.

Classification	Parameters	Isgur-Karl (Model I)	Chiral (Model II)
Re-adjusted	$m_{ud}$ (MeV)	313	360
	$m_s$ (MeV)	585	560
	K (MeV fm <sup>-2</sup> )	336	224
	$\beta$ (fm)	0.32	0.08
	$\alpha_0$	6.82	5.21
Fixed	$\Lambda_0$ (fm <sup>-1</sup> )	0.187	0.187
	$\mu_0$ (fm <sup>-1</sup> )	0.113	0.113
	$\Lambda_\pi$ (fm <sup>-1</sup> )	—	4.2
	$\Lambda_\sigma$ (fm <sup>-1</sup> )	—	4.2
	$\Lambda_K$ (fm <sup>-1</sup> )	—	5.2
	$\Lambda_\eta$ (fm <sup>-1</sup> )	—	5.2
	$m_\pi$ (fm <sup>-1</sup> )	—	0.70
	$m_K$ (fm <sup>-1</sup> )	—	2.51
	$m_\eta$ (fm <sup>-1</sup> )	—	2.77
	$m_\sigma$ (fm <sup>-1</sup> )	—	3.72
	$\theta_P$ (°)	—	-15
	$g_{ch}^2/4\pi$	—	0.54

and chiral quark model are listed in Table II, in which five parameters are re-adjusted to fit the light baryon spectrum. Other parameters  $\Lambda_\pi$ ,  $\Lambda_\sigma$ ,  $\Lambda_\eta$ ,  $\Lambda_K$ ,  $\theta_P$ ,  $\Lambda_0$  and  $\mu_0$ , which are fixed by fitting the meson spectra, are taken from Ref. [49].

### III. SIX-BODY CONFINEMENT POTENTIALS IN THE FLUX TUBE MODEL

In the flux tube model it is assumed that the color-electric flux is confined to narrow, string-like tubes joining quarks. A flux tube starts from every quark and ends at an anti-quark or a Y-shaped junction, where three flux tubes annihilate or are created [31]. In general, a state with  $N + 1$ -particles can be generated by replacing a quark or an anti-quark in an  $N$ -particles state by a Y-shaped junction and two quarks or two anti-quarks.

The  $q^3\bar{q}^3$  systems have been studied in the usual constituent quark model including a two-body confinement potential proportional to a color factor, no bound state is found for non-strange system [13, 60]. Vijande *et al* recently studied the stability of hexaquark states ( $q^6$  and  $q^3\bar{q}^3$ ) in the string confinement and found that the ground states of  $Q^3\bar{q}^3$  are stable against disintegrating into two color singlet baryons [61]. For  $q^3\bar{q}^3$  system, it can be consisted of a color singlet baryon and a color singlet anti-baryon as in the usual hadron degree of freedom description, but also of a color octet baryon and a color octet anti-baryon coupled to an overall color singlet six quark state. The former is named as hadronic molecule state, the latter is called hidden color channel and because of color confinement, the hidden color channel exists in the two-cluster overlap region only. These two structures are shown in Figs. 2 and 3, respectively. In general, a hexaquark system  $q^3\bar{q}^3$  should be a mixture of these two components. These two structures for  $q^3\bar{q}^3$  system are considered in the present work.

In Figs. 2 and 3,  $\mathbf{r}_\alpha$  represents the position coordinate of the quark  $q_\alpha$  (antiquark  $\bar{q}_\alpha$ ) which is denoted by a solid (hollow) dot, where  $\alpha = i, \dots, n$ ,  $(i, j, k)$  and  $(l, m, n)$  are cyclic indexes for (1,2,3) and (4,5,6), respectively.  $\mathbf{y}_\beta$  represents a junction, where  $\beta = 1, \dots, 4$ . A thin line connecting a quark and a junction represents a fundamental string, *i.e.*, a color triplet, a thick line connecting two junctions is for color sextet, octet or others, namely a compound string.

Within the flux tube model, the confinement potential for a hadronic molecule state can be written as

$$V_{min}^{CM} = K \left[ \left( \frac{\mathbf{r}_i - \mathbf{r}_j}{\sqrt{2}} \right)^2 + \left( \frac{2\mathbf{r}_k - \mathbf{r}_i - \mathbf{r}_j}{\sqrt{6}} \right)^2 + \left( \frac{\mathbf{r}_l - \mathbf{r}_m}{\sqrt{2}} \right)^2 + \left( \frac{2\mathbf{r}_n - \mathbf{r}_l - \mathbf{r}_m}{\sqrt{6}} \right)^2 \right]. \quad (22)$$

With respect to a hidden color state, the confinement potential has the following form

$$V^{CH} = K \left[ (\mathbf{r}_i - \mathbf{y}_1)^2 + (\mathbf{r}_j - \mathbf{y}_1)^2 + (\mathbf{r}_k - \mathbf{y}_2)^2 + (\mathbf{r}_n - \mathbf{y}_3)^2 + (\mathbf{r}_l - \mathbf{y}_4)^2 + (\mathbf{r}_m - \mathbf{y}_4)^2 + \kappa_{d_{12}}(\mathbf{y}_1 - \mathbf{y}_2)^2 + \kappa_{d_{23}}(\mathbf{y}_2 - \mathbf{y}_3)^2 + \kappa_{d_{34}}(\mathbf{y}_3 - \mathbf{y}_4)^2 \right]. \quad (23)$$

The string stiffness constant of an elementary or color triplet string is  $K$ , while  $K\kappa_{d_{ij}}$  is other compound

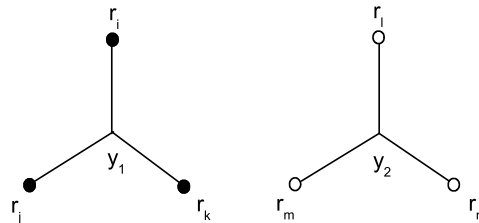


FIG. 2: Hadronic molecule structure.

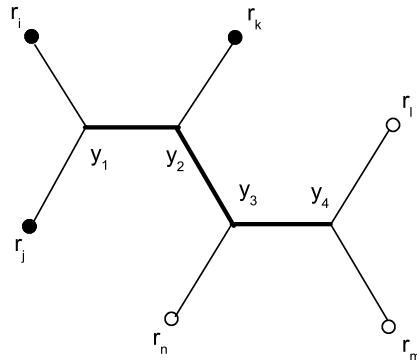


FIG. 3: Hidden color flux tube structure.

string stiffness. The compound string stiffness parameter  $\kappa_{d_{ij}}$  [62] depends on the color dimension,  $d_{ij}$ , of the string,

$$\kappa_{d_{ij}} = \frac{C_{d_{ij}}}{C_3}, \quad (24)$$

where  $C_{d_{ij}}$  is the eigenvalue of the Casimir operator associated with the  $SU(3)$  color representation  $d_{ij}$  on either end of the string, namely  $C_3 = \frac{4}{3}$ ,  $C_6 = \frac{10}{3}$  and  $C_8 = 3$ . In numerical calculations, the average  $\kappa_d$  for  $\kappa_{d_{ij}}$  is used for simplicity.

For given quark (antiquark) positions  $\mathbf{r}_\alpha$ , those junction coordinates  $\mathbf{y}_\beta$  are obtained by minimizing the confinement potential. By introducing the following set of canonical coordinates  $\mathbf{R}_i$ ,

$$\begin{aligned} \mathbf{R}_1 &= \frac{1}{\sqrt{2}}(\mathbf{r}_i - \mathbf{r}_j), & \mathbf{R}_2 &= \frac{1}{\sqrt{2}}(\mathbf{r}_l - \mathbf{r}_m) \\ \mathbf{R}_3 &= \frac{1}{\sqrt{12}}(\mathbf{r}_i + \mathbf{r}_j - 2\mathbf{r}_k - 2\mathbf{r}_n + \mathbf{r}_l + \mathbf{r}_m) \\ \mathbf{R}_4 &= \frac{1}{\sqrt{33 + 5\sqrt{33}}}(\mathbf{r}_i + \mathbf{r}_j - w_1\mathbf{r}_k + w_1\mathbf{r}_n - \mathbf{r}_l - \mathbf{r}_m) \\ \mathbf{R}_5 &= \frac{1}{\sqrt{33 - 5\sqrt{33}}}(\mathbf{r}_i + \mathbf{r}_j + w_2\mathbf{r}_k - w_2\mathbf{r}_n - \mathbf{r}_l - \mathbf{r}_m) \\ \mathbf{R}_6 &= \frac{1}{\sqrt{6}}(\mathbf{r}_i + \mathbf{r}_j + \mathbf{r}_k + \mathbf{r}_l + \mathbf{r}_m + \mathbf{r}_n), \end{aligned} \quad (25)$$

where  $w_1 = \frac{\sqrt{33+5}}{2}$  and  $w_2 = \frac{\sqrt{33-5}}{2}$ , the minimum of the

confinement potential takes the following form,

$$V_{min}^{CH} = K \left[ \mathbf{R}_1^2 + \mathbf{R}_2^2 + \frac{3\kappa_d}{2+3\kappa_d} \mathbf{R}_3^2 + \frac{2\kappa_d(\kappa_d+w_3)}{2\kappa_d^2+7\kappa_d+2} \mathbf{R}_4^2 + \frac{2\kappa_d(\kappa_d+w_4)}{2\kappa_d^2+7\kappa_d+2} \mathbf{R}_5^2 \right], \quad (26)$$

where  $w_3 = \frac{7+\sqrt{33}}{4}$  and  $w_4 = \frac{7-\sqrt{33}}{4}$ . Clearly this confinement potential is multibody interaction rather than the sum of two-body one in the sense that a move of a quark may affect flux tubes connecting pattern.

When two clusters  $q^3$  and  $\bar{q}^3$  separate in a long distance, a baryon and an antibaryon should be a dominant component of a hexaquark  $q^3\bar{q}^3$  system because other hidden color flux tube structures are suppressed due to the confinement. On the other hand, if the separation is intermediate, a hadronic molecule state may be formed if the attractive force between a baryon and an antibaryon is strong enough. When the two quark-clusters are close enough to be within the range of confinement (about 1 fm), all possible flux tube structures will appear due to the excitation and rearrangement of flux tubes. In this case, the confinement potential of a hexaquark system  $q^3\bar{q}^3$  should be taken to be the minimum of two flux tube structures. It reads

$$V_{min}^C = \min [V_{min}^{CM}, V_{min}^{CH}]. \quad (27)$$

#### IV. NUMERICAL RESULTS AND DISCUSSIONS

The flux tube structure specifies how the colors of quarks and anti-quarks are coupled to form an overall color singlet. Therefore, the model wavefunction with defined quantum numbers  $I_T$  and  $J_T$  can be expressed as,

$$\Psi_{I_T, J_T}^{q^3\bar{q}^3} = \sum c_\xi \left[ \left[ \Phi_{c_1 I J}^{q^3} \Phi_{c_2 I' J'}^{\bar{q}^3} \right]_\xi F_{L'}(\mathbf{X}) \right]_{I_T J_T} \quad (28)$$

$\Phi_{c_1 I J}^{q^3}$  and  $\Phi_{c_2 I' J'}^{\bar{q}^3}$  are cluster wavefunctions of colorful or colorless baryon and anti-baryon, respectively. The spatial wavefunctions are the same as those of baryons shown before,  $[\dots]_\xi$  represents all the needed coupling: color, isospin and spin coupling.  $F_{L'}(\mathbf{X})$  is the relative orbital wavefunction between  $q^3$  and  $\bar{q}^3$  clusters. All the possible channels are taken into account in our multichannel coupling calculation, the details can be seen in Table III. The Jacobi coordinates for a  $q^3\bar{q}^3$  system are shown in Fig. 4, which can be expressed as

$$\begin{aligned} \mathbf{r}_{ij} &= \mathbf{r}_i - \mathbf{r}_j, \quad \mathbf{R}_k = \mathbf{r}_k - \frac{\mathbf{r}_i + \mathbf{r}_j}{2}, \\ \mathbf{r}_{lm} &= \mathbf{r}_l - \mathbf{r}_m, \quad \mathbf{R}_n = \mathbf{r}_n - \frac{\mathbf{r}_l + \mathbf{r}_m}{2}, \\ \mathbf{X} &= \frac{\mathbf{r}_i + \mathbf{r}_j + \mathbf{r}_k}{3} - \frac{\mathbf{r}_l + \mathbf{r}_m + \mathbf{r}_n}{3}. \end{aligned} \quad (29)$$

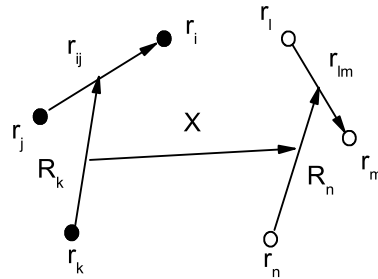


FIG. 4: Jacobi ordinates for a  $q^3\bar{q}^3$  system.

Using GEM, the relative orbital wavefunction  $F_{L'}(\mathbf{X})$  can be written as,

$$F_{L'}(\mathbf{X}) = \sum_{N'=1}^{N'_{max}} c_{N'} N_{N'L'} X^{L'} e^{-\nu_{N'} X^2} Y_{L'M'}(\hat{\mathbf{X}}) \quad (30)$$

Now we turn to the numerical calculations on  $q^3\bar{q}^3$  systems. In Model I and II, where a six-body confinement potential is used, all the model parameters are fixed by fitting the ground state baryon spectrum, no new parameter is introduced in the six-body calculation. The eigenvalues and eigenfunctions of the  $q^3\bar{q}^3$  states can be obtained by solving the following six-body Schrödinger equation

$$(H_6 - E)\Psi_{I_T J_T}^{q^3\bar{q}^3} = 0 \quad (31)$$

with Rayleigh-Ritz variational principle. The calculated results are converged with  $n_{max}=5$ ,  $N_{max} = 5$  and  $N'_{max} = 5$ . Minimum and maximum ranges of the bases are 0.3 fm and 2.0 fm for coordinates  $\mathbf{r}$ ,  $\mathbf{R}$  and  $\mathbf{X}$ , respectively.

The lowest multichannel coupling results for all possible quantum numbers are listed in Table III, the superscript and subscript of  $N(\Delta)$  represent spin quantum number and color dimensions, respectively.  $E_T(B + \bar{B})$  is the threshold of decaying into a baryon and an antibaryon,  $\Delta E_I$  and  $\Delta E_{II}$  are binding energies of hexaquark states  $q^3\bar{q}^3$  in Model I and Model II, respectively. It can be seen from Table III that the states with  $I^G J^{PC} = 0^- 3^{--}$ ,  $1^+ 3^{--}$  and  $3^+ 1^{--}$  are bound states only in Model II. For other states almost the same qualitative results are obtained in two models. It suggests that there are some bound states below the lowest threshold in the present calculations. The states with  $I^G J^{PC} = 0^+ 0^{-+}$  and  $1^- 0^{-+}$  are stable against disintegrating into  $N + \bar{N}$ . The states with  $I^G J^{PC} = 1^- 2^{-+}$ ,  $2^- 1^{--}$  and  $2^+ 2^{-+}$  are stable against disintegrating into  $N + \bar{\Delta}$  or  $\bar{N} + \Delta$ , but decay to  $N\bar{N}\pi$  is allowed. The states with  $I^G J^{PC} = 0^+ 2^{-+}$ ,  $2^+ 0^{-+}$  and  $3^+ 0^{-+}$  are stable against disintegrating into  $\Delta + \bar{\Delta}$ , decaying to  $N\bar{N}\pi\pi$  is allowed. The states with  $I^G J^{PC} = 0^- 1^{--}$ ,  $1^+ 1^{--}$ ,  $2^- 3^{--}$ ,  $3^- 2^{-+}$  and  $3^+ 3^{--}$  states are not bound both

TABLE III: Binding energies of lowest  $q^3\bar{q}^3$  states with all possible quantum numbers in Model I and II. (unit: MeV)

$I^G J^{PC}$	Coupled channels	$E_T(B + \bar{B})$	$\Delta E_I$	$\Delta E_{II}$
$0^+ 0^{-+}$	$N_8^{\frac{1}{2}} \bar{N}_8^{\frac{1}{2}}, \Delta_8^{\frac{1}{2}} \bar{\Delta}_8^{\frac{1}{2}}, N_8^{\frac{3}{2}} \bar{N}_8^{\frac{3}{2}}, N\bar{N}, \Delta\bar{\Delta}$	939+939	-44	-34
$0^- 1^{--}$	$N_8^{\frac{1}{2}} \bar{N}_8^{\frac{1}{2}}, N_8^{\frac{1}{2}} \bar{N}_8^{\frac{3}{2}}, \Delta_8^{\frac{1}{2}} \bar{\Delta}_8^{\frac{1}{2}}, N_8^{\frac{3}{2}} \bar{N}_8^{\frac{1}{2}}, N_8^{\frac{3}{2}} \bar{N}_8^{\frac{3}{2}}, N\bar{N}, \Delta\bar{\Delta}$	939+939	0	0
$0^+ 2^{-+}$	$N_8^{\frac{1}{2}} \bar{N}_8^{\frac{3}{2}}, N_8^{\frac{3}{2}} \bar{N}_8^{\frac{1}{2}}, N_8^{\frac{3}{2}} \bar{N}_8^{\frac{3}{2}}, \Delta\bar{\Delta}$	1232+1232	-269	-200
$0^- 3^{--}$	$N_8^{\frac{1}{2}} \bar{N}_8^{\frac{3}{2}}, \Delta\bar{\Delta}$	1232+1232	0	-58
$1^- 0^{-+}$	$N_8^{\frac{1}{2}} \bar{N}_8^{\frac{1}{2}}, N_8^{\frac{1}{2}} \bar{\Delta}_8^{\frac{1}{2}}, \Delta_8^{\frac{1}{2}} \bar{N}_8^{\frac{1}{2}}, \Delta_8^{\frac{1}{2}} \bar{\Delta}_8^{\frac{1}{2}}, N_8^{\frac{3}{2}} \bar{N}_8^{\frac{1}{2}}, N\bar{N}, \Delta\bar{\Delta}$	939+939	-44	-5
$1^+ 1^{--}$	$N_8^{\frac{1}{2}} \bar{N}_8^{\frac{1}{2}}, N_8^{\frac{1}{2}} \bar{\Delta}_8^{\frac{1}{2}}, N_8^{\frac{1}{2}} \bar{N}_8^{\frac{3}{2}}, \Delta_8^{\frac{1}{2}} \bar{N}_8^{\frac{1}{2}}, \Delta_8^{\frac{1}{2}} \bar{\Delta}_8^{\frac{1}{2}}, \Delta_8^{\frac{1}{2}} \bar{N}_8^{\frac{3}{2}}, N_8^{\frac{3}{2}} \bar{N}_8^{\frac{1}{2}}, N_8^{\frac{3}{2}} \bar{\Delta}_8^{\frac{1}{2}}, N_8^{\frac{3}{2}} \bar{N}_8^{\frac{3}{2}}, N\bar{N}, N\bar{\Delta}, \Delta\bar{N}, \Delta\bar{\Delta}$	939+939	0	0
$1^- 2^{-+}$	$N_8^{\frac{1}{2}} \bar{N}_8^{\frac{3}{2}}, \Delta_8^{\frac{1}{2}} \bar{N}_8^{\frac{3}{2}}, N_8^{\frac{3}{2}} \bar{N}_8^{\frac{1}{2}}, N_8^{\frac{3}{2}} \bar{N}_8^{\frac{3}{2}}, N\bar{\Delta}, \Delta\bar{N}, \Delta\bar{\Delta}$	939+1232	-7	-71
$1^+ 3^{--}$	$N_8^{\frac{3}{2}} \bar{N}_8^{\frac{3}{2}}, \Delta\bar{\Delta}$	1232+1232	0	-44
$2^+ 0^{-+}$	$N_8^{\frac{1}{2}} \bar{\Delta}_8^{\frac{1}{2}}, \Delta_8^{\frac{1}{2}} \bar{N}_8^{\frac{1}{2}}, \Delta_8^{\frac{1}{2}} \bar{\Delta}_8^{\frac{1}{2}}, \Delta\bar{\Delta}$	1232+1232	-88	-87
$2^- 1^{--}$	$N_8^{\frac{1}{2}} \bar{\Delta}_8^{\frac{1}{2}}, \Delta_8^{\frac{1}{2}} \bar{N}_8^{\frac{1}{2}}, \Delta_8^{\frac{1}{2}} \bar{\Delta}_8^{\frac{1}{2}}, \Delta_8^{\frac{1}{2}} \bar{N}_8^{\frac{3}{2}}, N_8^{\frac{3}{2}} \bar{\Delta}_8^{\frac{1}{2}}, N\bar{\Delta}, \Delta\bar{N}, \Delta\bar{\Delta}$	939+1232	-13	-108
$2^+ 2^{-+}$	$N_8^{\frac{3}{2}} \bar{\Delta}_8^{\frac{1}{2}}, \Delta_8^{\frac{1}{2}} \bar{N}_8^{\frac{3}{2}}, N\bar{\Delta}, \Delta\bar{N}, \Delta\bar{\Delta}$	939+1232	-7	-34
$2^- 3^{--}$	$\Delta\bar{\Delta}$	1232+1232	0	0
$3^- 0^{-+}$	$\Delta_8^{\frac{1}{2}} \bar{\Delta}_8^{\frac{1}{2}}, \Delta\bar{\Delta}$	1232+1232	-88	-76
$3^+ 1^{--}$	$\Delta_8^{\frac{1}{2}} \bar{\Delta}_8^{\frac{1}{2}}, \Delta\bar{\Delta}$	1232+1232	0	-67
$3^- 2^{-+}$	$\Delta\bar{\Delta}$	1232+1232	0	0
$3^+ 3^{--}$	$\Delta\bar{\Delta}$	1232+1232	0	0

in two models. The multibody confinement potential based on the color flux tube picture can give more attraction than the additive two-body confinement interaction which is proportional to color factors used in early multi-quark state calculations, due to avoiding the appearance of the anti-confinement in a color symmetrical quark or antiquark pair. In fact one gluon exchange and one boson exchange interaction also provide attractive interaction for some states [61].

For the state  $I^G J^{PC} = 0^+ 0^{-+}$ , the wavefunction can be separated into two groups,  $N\bar{N} + N_8\bar{N}_8$  and  $\Delta\bar{\Delta} + \Delta_8\bar{\Delta}_8$ . In Model I, there is no interaction between  $N\bar{N} + N_8\bar{N}_8$  and  $\Delta\bar{\Delta} + \Delta_8\bar{\Delta}_8$  due to the absence of boson exchange term. The states  $N\bar{N} + N_8\bar{N}_8$  and  $\Delta\bar{\Delta} + \Delta_8\bar{\Delta}_8$  have the lowest energies 1834 MeV and 2376 MeV, respectively. However,  $N\bar{N} + N_8\bar{N}_8$  and  $\Delta\bar{\Delta} + \Delta_8\bar{\Delta}_8$  are

mixed in Model II because there is interaction among them due to one boson exchange. But the mixing effect is not large. The energies of  $N\bar{N} + N_8\bar{N}_8$  and  $\Delta\bar{\Delta} + \Delta_8\bar{\Delta}_8$  are 1865 MeV and 2384 MeV in the Model II if the mixing effect among two groups is neglected. The mixing moves the energies of  $N\bar{N} + N_8\bar{N}_8$  to 1844 MeV and  $\Delta\bar{\Delta} + \Delta_8\bar{\Delta}_8$  to 2388 MeV.  $N\bar{N} + N_8\bar{N}_8$  and  $\Delta\bar{\Delta} + \Delta_8\bar{\Delta}_8$  are bound states because their energies are lower than the corresponding thresholds of  $N\bar{N}$  and  $\Delta\bar{\Delta}$  in these two models. The masses of  $N\bar{N} + N_8\bar{N}_8$  and  $\Delta\bar{\Delta} + \Delta_8\bar{\Delta}_8$  states are close to the masses of newly observed states  $X(1835)$  and  $X(2370)$ , so it is possible to interpret the main components of  $X(1835)$  and  $X(2370)$  as  $N\bar{N} + N_8\bar{N}_8$  and  $\Delta\bar{\Delta} + \Delta_8\bar{\Delta}_8$  in the present calculation, respectively. However, another state  $X(2120)$  observed by BES-III can not be described in the present calculations.

TABLE IV: Rms for  $N\bar{N} + N_8\bar{N}_8$  and  $\Delta\bar{\Delta} + \Delta_8\bar{\Delta}_8$  (fm).

Model	Distances	$\langle \mathbf{R}_{qqq}^2 \rangle^{\frac{1}{2}}$	$\langle \mathbf{R}_{\bar{q}\bar{q}\bar{q}}^2 \rangle^{\frac{1}{2}}$	$\langle \mathbf{X}^2 \rangle^{\frac{1}{2}}$
Model I	$N\bar{N} + N_8\bar{N}_8$	0.61	0.61	0.51
	$\Delta\bar{\Delta} + \Delta_8\bar{\Delta}_8$	0.65	0.65	0.60
Model II	$N\bar{N} + N_8\bar{N}_8$	0.66	0.66	0.58
	$\Delta\bar{\Delta} + \Delta_8\bar{\Delta}_8$	0.71	0.71	0.66

Using the wavefunctions of  $N\bar{N} + N_8\bar{N}_8$  and  $\Delta\bar{\Delta} + \Delta_8\bar{\Delta}_8$ , the root mean square radii (rms) of the two states with  $I^G J^{PC} = 0^+ 0^{-+}$  are calculated and given in Table IV, where

$$\mathbf{R}_{qqq} = \mathbf{r}_i - \frac{\mathbf{r}_j + \mathbf{r}_k}{3}$$

and

$$\mathbf{R}_{\bar{q}\bar{q}\bar{q}} = \mathbf{r}_l - \frac{\mathbf{r}_m + \mathbf{r}_n}{3}.$$

It can be seen from Table IV that the radii are small and very close in two models. The two clusters  $q^3$  and  $\bar{q}^3$  are highly overlapped, therefore the main components of  $X(1835)$  and  $X(2370)$  are not loose hadronic molecule states but compact hexaquark states with three-dimensional configurations similar to rugby ball in the present calculations.

All hidden color components can not decay into two colorful hadrons directly due to color confinement.  $X(1835)$  and  $X(2370)$  must transform back into three color singlet mesons by means of breaking and rejoining flux tubes before decaying into  $\eta'\pi^+\pi^-$ . This decay mechanism is similar to compound nucleus formation and therefore should induce a resonance which is named as a ‘‘color confined, multi-quark resonance’’ state [63] in our models. It is different from all of those microscopic resonances discussed by S. Weinberg [64]. Bicudo and Cardoso studied tetraquark states using the triple flip-flop potential including two meson-meson potentials and the tetraquark four-body potential. They also found plausibly the existence of resonances in which the tetraquark

component originated by a flip-flop potential is the dominant one [65].

## V. SUMMARY

By using high precision few-body calculation method, GEM, non-strange hexaquark states  $q^3\bar{q}^3$  including  $B_8\bar{B}_8$  and  $B\bar{B}$  components are studied in flux tube models, extended chiral quark model (Model II) and Isgur-Karl model (Model I), with a six-body confinement potential. In the present version of flux tube models, the system will automatically choose its favorable configuration by means of the recombination of the flux tube when the quarks and anti-quarks are moving. The flux tube models which includes multibody confinement potential generally give more attraction than the two-body confinement models with color factors that was used in the early multi-quark calculations. The two types of flux tube models give similar results for non-strange hexaquark system. Our calculations suggest that some states are stable against decaying into a baryon and an anti-baryon.

One gluon exchange and one boson exchange interaction also provide attractive interaction for some states, and therefore should be taken into account altogether.

The states  $X(1835)$  and  $X(2370)$  can be explained as  $N\bar{N}+N_8\bar{N}_8$  and  $\Delta\bar{\Delta}+\Delta_8\bar{\Delta}_8$  bound states in the flux tube models, the main components are compact hexaquark states  $N_8\bar{N}_8$  and  $\Delta_8\bar{\Delta}_8$ , respectively. Such states should be color confinement resonances with three-dimensional configurations similar to rugby ball.  $X(2120)$  can not be accommodated in this model. We admit that this analysis is based on the mass calculation only, the decay properties of these states have to be invoked to check the assignment, which is left for future.

## Acknowledgments

This work is supported partly by the National Science Foundation of China under Contract Nos. 11047140, 11175088, 11035006, 11047023, and the Ph.D Program Funds of Chongqing Jiaotong University.

- 
- [1] J. Z. Bai et al. (BES Collaboration), Phys. Rev. Lett. **91**, 022001 (2003).
  - [2] M. Ablikim et al. (BES Collaboration), Phys. Rev. Lett. **95**, 262001 (2005).
  - [3] M. Ablikim et al. (BES Collaboration), Phys. Rev. Lett. **106**, 072002 (2011).
  - [4] A. Datta and P. J. O'Donnell, Phys. Lett. B **567**, 273 (2006).
  - [5] G. J. Ding and M. L. Yan, Phys. Rev. C **72**, 015208 (2005).
  - [6] C. S. Gao and S. L. Zhu, Commun. Theor Phys. **42**, 844 (2004).
  - [7] N. Kochelev and D. P. Min, Phys. Lett. B **633**, 283 (2006).
  - [8] X. G. He, X. Q. Li, X. Liu and J. P. Ma, Eur. Phys. J. C **49**, 731 (2007)
  - [9] B. A. Li, Phys. Rev. D **74**, 034019 (2006).
  - [10] G. J. Ding and M. L. Yan, Eur. Phys. J. A **28**, 351 (2006).
  - [11] C. Liu, Eur. Phys. J. C **53**, 413 (2008).
  - [12] T. Huang and S. L. Zhu, Phys. Rev. D **73**, 014023 (2006).
  - [13] D. R. Entem and F. Fernández, Phys. Rev. C **73**, 045214 (2006).
  - [14] J. S. Yu, Z. F. Sun, X. Liu and Q. Zhao, Phys. Rev. D **83**, 114007 (2011).
  - [15] P. Maris and C. R. Roberts, Int. J. Mod. Phys. E **12**, 297 (2003).
  - [16] N. Ishii, S. Aoki, and T. Hatsuda, Phys. Rev. Lett. **99**, 022001 (2007).
  - [17] T. T. Takahashi and Y. Kanada-En'yo, Phys. Rev. D **82**, 094506 (2010).
  - [18] T. Inoue, N. Ishii and S. Aoki et al (HAL QCD Collaboration), Phys. Rev. Lett. **106**, 162002 (2011).
  - [19] N. Ishii, AIP Conf. Proc. **1355**, 206-213 (2011).
  - [20] S. Godfrey and J. Napolitano, Rev. Mod. Phys. **71**, 5 (1999).
  - [21] J. Weinstein and N. Isgur, Phys. Rev. D **41**, 2238 (1990).
  - [22] G. Feinberg and J. Sucher, Phys. Rev. D **20**, 1717 (1979)
  - [23] O. W. Greenberg and H. J. Lipkin, Nucl. Phys. A **370**, 349 (1981).
  - [24] J. Weinstein and N. Isgur, Phys. Rev. Lett. **48**, 659 (1982).
  - [25] M. Oka, Phys. Rev. D **31**, 2274 (1985).
  - [26] M. Oka and C. J. Horowitz, Phys. Rev. D **31**, 2773 (1985).
  - [27] H. J. Lipkin, Phys. Lett. B **113**, 490 (1982).
  - [28] O. W. Greenberg and J. Hietarinta, Phys. Lett. B **86**, 309 (1979).
  - [29] O. W. Greenberg and J. Hietarinta, Phys. Rev. D **22**, 993 (1980);
  - [30] D. Robson, Phys. Rev. D **35**, 1018 (1987).
  - [31] N. Isgur and J. Paton, Phys. Rev. D **31**, 2910 (1985).
  - [32] J. L. Ping, C. R. Deng, F. Wang and T. Goldman, Phys. Lett. B **659**, 607 (2008).
  - [33] C. R. Deng, J. L. Ping, F. Wang and T. Goldman, Phys. Rev. D **82**, 074001 (2010).
  - [34] F. Wang and C. W. Wong, Nuovo Cimento A **86**, 283 (1985).
  - [35] V. Dmitrasinovic, Phys. Rev. D **67**, 114007 (2003).
  - [36] C. Alexandrou, P. De Forcrand and A. Tsapalis, Phys. Rev. D **65**, 054503 (2002).
  - [37] T. T. Takahashi, H. Suganuma, Y. Nemoto and H. Matsu-furu, Phys. Rev. D **65**, 114509 (2002).
  - [38] F. Okiharu, H. Suganuma and T. T. Takahashi, Phys. Rev. D **72**, 014505 (2005).
  - [39] F. Okiharu, H. Suganuma and T. T. Takahashi, Phys. Rev. Lett. **94**, 192001 (2005).
  - [40] J. L. Ping, F. Wang and T. Goldman, Nucl. Phys. A **657**, 95 (1999).
  - [41] A. Valcarce, H. Garcilazo, F. Fernández and P. González, Rep. Prog. Phys **68**, 965 (2005).

- [42] T. Goldman and S. Yankielowicz, Phys. Rev. D **12**, 2910 (1975).
- [43] C. R. Deng, J. L. Ping and F. Wang, arXiv: 1202.4169 (hep-ph).
- [44] E. Hiyama, Y. Kino and M. Kamimura, Prog. Part. Nucl. Phys. **51** 223 (2003).
- [45] N. Isgur and G. Karl, Phys. Rev. D **18**, 4187 (1978).
- [46] N. Isgur and G. Karl, Phys. Rev. D **19**, 2653 (1979).
- [47] N. Isgur and G. Karl, Phys. Rev. D **20**, 1191 (1979).
- [48] N. Isgur and G. Karl, Phys. Rev. Lett. **48**, 659 (1982).
- [49] J. Vijande, F. Fernandez and A. Valcarce, J. Phys. G **31**, 481 (2005).
- [50] J. Weinstein, N. Isgur, Phys. Rev. D **27**, 588 (1983).
- [51] I. T. Obukhovskiy and A. M. Kusainov, Phys. Lett. B **238**, 142 (1990).
- [52] F. Fernández, A. Valcarce, U. Straub and A. Faessler, J. Phys. G: Nucl. Part. Phys. **19**, 2013 (1993).
- [53] A. Valcarce, P. González, F. Fernández and V. Vento, Phys. Lett. B **367**, 35 (1996).
- [54] L. Y. Glozman and D. O. Riska, Phys. Rep. **268**, 263 (1996).
- [55] Y. Fujiwara, C. Nakamoto and Y. Suzuki, Phys. Rev. C **54**, 2180 (1996).
- [56] Y. Fujiwara, M. Khono, C. Nakamoto and Y. Suzuki, Phys. Rev. C **64**, 054001 (2001).
- [57] Y. Fujiwara, K. Miyagawa, M. Khono, Y. Suzuki and C. Nakamoto, Nucl. Phys. A **737**, 243 (2004).
- [58] M. D. Scadron, Phys. Rev. D **26**, 239 (1982).
- [59] F. Bissey, F. G. Cao, A. R. Kitson, and A. I. Signal et al, Phys. Rev. D **76**, 114512 (2007).
- [60] H. X. Huang, H. R. Pang and J. L. Ping, Mod. Phys. Lett. A **26**, 1231 (2011).
- [61] J. Vijande, A. Valcarce and J. M. Richard, Phys. Rev. D **85**, 014019 (2012).
- [62] G. S. Bali, Phys. Rev. D **62**, 114503 (2000).
- [63] Fan Wang, J. L. Ping, H. R. Pang and L. Z. Chen, Nucl. Phys. A **790**, 493c (2007).
- [64] S. Weinberg, *The Quantum Theory of Fields*, (Cambridge University Press, 1995), V.I, p.159.
- [65] P. Bicudo and M. Cardoso, Phys. Rev. D **83**, 094010 (2011).